Biointerface Research in Applied Chemistry
Platinum Open Access Journal (ISSN: 2069-5837)

Article
Volume 11, Issue 1, 2021, 7785 - 7793
https://doi.org/10.33263/BRIAC111.77857793

Exploring Structural, Morphological, and Magnetic Properties of Zinc Nickel Ferrites Systems Nanocomposites

Arthur Charles Prabakar [1], Govindarasu Killivalavan [1], Dhananjayan Sivakumar [2], K. Chandra Babu Naidu [3], Balaraman Sathyaseelan [4,*], Krishnamoorthy Senthilnathan [5], Iruson Baskaran [6], Elayaperumal Manikandan [7], M. Balaraju [8]

1 Research and Development Centre, Bharathiar University, Coimbatore-641046, India
2 Department of Physics, Sree Krishna College of Engineering, Unai, Anaicut-632101, Tamilnadu, India
3 Department of Physics, GITAM Deemed to be University, Bangalore-562163, Karnataka, India
4 Department of Physics, University College of Engineering Arni, Anna University Chennai, Arni 632326, Tamil Nadu, India
5 Photonics Division, School of Advanced Sciences, VIT University, Vellore, 632014, Tamil Nadu, India
6 Department of Physics Arignar Anna Government Arts College, Cheyyar 604407, Tamil Nadu, India
7 Department of Physics, Thiruvalluvar University College of Arts and Science, Thennangur Village, Vandavasi Taluk, Tiruvannamalai District 604408, India
8 Department of Chemistry, PSC & KVSC Govt. Degree College, Nandyal, Kurnool-518502, A.P., India
* Correspondence: bsseelan03@gmail.com;

Scopus Author ID 35734996700
Received: 26.05.2020; Revised: 1.07.2020; Accepted: 2.07.2020; Published: 4.07.2020

Abstract: The formation of Zinc Nickel Ferrites Systems Nanocomposites (ZNFONCs) through Ethylene glycol (PEG) surfactant was achieved by chemical co-precipitation technique. Their structure, shape, and constituents were investigated by X-ray diffraction, dispersion, and scanning electron microscopy. The photocatalyst effect of Zinc-Nickel ferrite system Nanocomposites was determined by methyl Blue (MB), when exposed to ultraviolet light. Magnetization estimation by vibrating magnetometer at room temperature is an additional effort in the present work.

Keywords: Zinc nickel ferrite system; Chemical synthesis; Microstructure; Magnetic estimations.

1. Introduction

Nanocomposites have earned sufficient attraction among materials, due to their nanocrystal properties which purely rely on their composition and dimension [1-5]. Photocatalytic activity on semiconductors has aroused interest because the technique is one of the most reliable and effective means for the disposal of organic impurities [6-8]. Due to the high probability of altering their attributes through cation splitting or atomic replacement into the tetrahedral or octahedral region, Cubic ferrite nanoparticles have a wide application [9-11]. Their formula is $M^{2+}Fe_2^{3+}O_4^{2-}$, where M can be Co^{2+}, Zn^{2+}, Ni^{2+}. Apart from spin-filtering [12] and multiferroic devices [13-14], Identification, diagnosis, and solution have been disclosed in biomedicine. Magnetic nanoparticles have enhanced potential because of its ample application in data gathering, diagnostics, Ferrofluid dynamics, etc., [15-18]. This is significant because the characteristics of nanoparticles are distinct from their parental sample [19]. Zinc substituted ferrites (Ni-Zn) are found to be sensitive to temperature. Ferrofluids formed by these ferrites are excellent material, in heat exchangers by converting magnetic into caloric energy [20-22].

Different preparation approaches, such as sol-gel pyrolysis [23] ball milling [24] and microemulsion [25] was commonly used in manufacturing nanoparticles. But co-precipitation is inexpensive in fabricating fine particles. The characteristics of nanoparticles are the foci of researchers due to their dimension and crystallinity. The Zn-Ni ferrites making and attribution have been cataloged only to a certain threshold limit. In high-density, single-domain Nickel ferrite particle finds many applications. It has also been reported, by different stirring speeds, the size of nanoparticles can be maintained [26, 27]. The present work analyses the synthesis, structural, morphological, and parameters of the Zinc-Nickel ferrite system arrived by means of chemical co-precipitation.

2. Materials and Methods

2.1. Synthesis of Zinc-Nickel ferrite system Nanocomposites.

The chemicals used are of high analytical quality and are used without cleansing. In a classical synthesis procedure, $Ni(NO_3)_2.6H_2O$, $Zn(NO_3)_2.6H_2O$ and $Fe(NO_3)_3.9H_2O$ were dissolved in water. The mixture was heated to a temperature of 45ºC for 15 min. Later, the metal nitrates precursor solution was added with sodium hydroxide (NaOH) along with continuous stirring. The reaction was carried out at 80ºC. The reagent was added in drops into the metal solution, with constant stirring till co-precipitation occur and doing so the pH value reaches 10. The reaction temperature was maintained at 85°C for 45 min.

The composites were cooled, and the precipitate was filtered and cleansed with pure ethanol and water. To remove the water contents, the sample was dried for 24 hrs at a temperature of 110 °C. The powder was made homogeneous using agate mortar. It was then annealed at two different temperatures, 500°C and 600°C. Finally, the annealed powder was subjected to different analysis techniques. The studies on the shape and distribution of zinc-nickel ferrite system nanocomposites using high resolving power transmission electron microscope, instrument operated at a high voltage of 120 kV and also subjected to high resolution scanning electron view (HRSEM).

The zinc-nickel ferrite system Nanocomposites constituents were empowered using EDAX. The dynamics and structural aspects of the obtained zinc-nickel ferrite system Nanocomposites were obtained by Fourier transformation infrared spectroscopy. The vibrational measurements were studied using the fiber optics LED. Using the VSM lakeshore-7404, magnetic parameters were analyzed, with a magnetic field of 10 kOe.

2.2. Photocatalytic phenomenon.

The methylene Blue (MB) photo decay was examined to assess the photocatalytic activities of the Zinc-Nickel ferrite system nanocomposites. The process is achieved with exposure to ultraviolet light. The activity was carried with 0.1 g of Zinc-Nickel ferrite in 50 mL methylene blue. The adsorption equilibrium was attained by oxygenated the sample for 30 min. The powder was placed inside a light reactor with mercury lamps, which act as the source for UV radiation. A fraction of the mixture was collected at specific periods during the exposure and centrifugation. Finally, they were subjected to UV–Vis spectra analysis.

3. Results and Discussion

3.1. Structural and Crystalline nature of the Zn-Ni ferrite system Nanocomposites.

To explore the crystalline nature of the ferrite nano composites, XRD (Fig. 1) were engaged. Figure.1 shows XRD graphs of the prepared Zinc-Nickel ferrite system at different calcination temperatures (500 and 600°C). From the observed results, the zinc-nickel ferrite system exhibit intense diffraction peaks implying their crystalline and nano behavior.

The peak 2θ values of 30.26°, 36.6°,48.61°, 53.19°, and 61.0° are indexed as (220), (311), (400), (440) and (200) planes are in firm agreement with the outcomes of samples through the JCPDS (card no.82-1042) confirming the formation of a cubic phase with a ferrite system structure [28-29]. As the phase of zinc-nickel ferrite system crystallites increases, the shape of the Nanocomposites is found to be different at varying annealing temperatures (As-prepared, 500 °C and 600 °C) with an increase in the grain size. This can be well interpreted with respect to the cation ratio. The radius of Ni^{2+} ion (0.69Å) is intermediate to Fe^{2+} (0.74 Å) and Fe^{3+} (0.64 Å), which confirms that theNi^{2+}ions only prefer octahedral space.

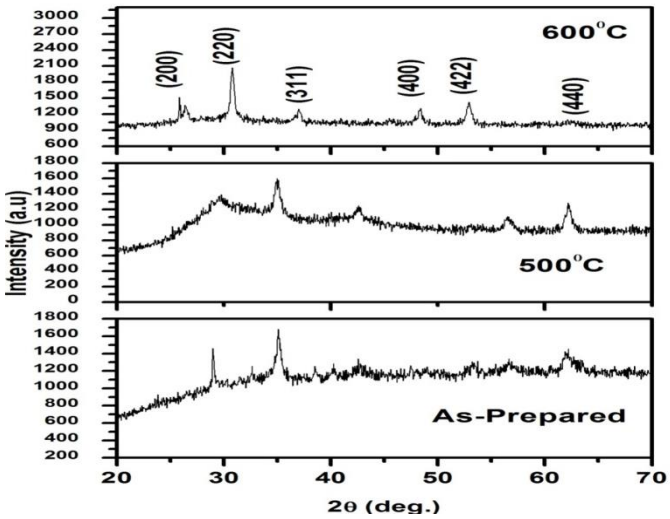

Figure 1. Powder XRD of Zinc-Nickel Ferrites Systems (ZNFO NCs) Nanocomposites.

3.2. Morphology and fundamental aspects of the Zinc-Nickel ferrite system Nanocomposites.

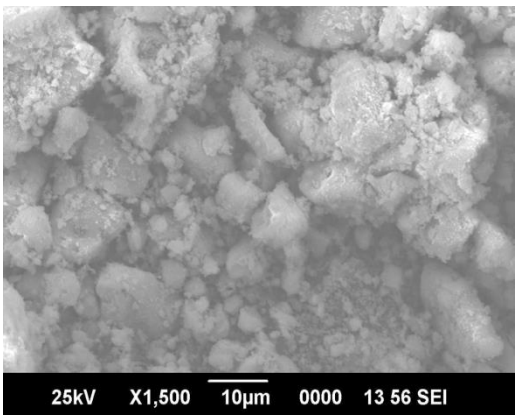

Figure 2. SEM images of Zinc Nickel Ferrites Systems (ZNFO NCs) Nanocomposites annealed at 600ºC.

HRSEM images reveal that the Zinc-Nickel ferrite system nanocomposites are tiny spheres (Fig. 2) at 600°C, and the clusters are arrayed into spherical forms. It is acknowledged

that the change in temperature exhibits a drastic change in size, shape, phase, and form of the nanocomposites. When particles alter from dense to thin distribution, the nature of the material tends to crystalline nature. The impact may be due to spin coupling and its magnetic behavior [30]. The EDAX spectrum and quantitative results of the zinc-nickel ferrite system nanocomposites are shown in Fig. (3). The EDAX spectra confirmed the presence of the constituents, i.e., Zinc (Zn), Nickel (Ni), Iron (Fe), and Oxygen (O) in the synthesized nanoparticles along with the trace impurities like Sodium (Na) and Chlorine (Cl).

The observed result from EDAX is in proximity to the XRD study. High-resolution TEM images of multi-crystalline nature of the zinc-nickel ferrite system nanocomposites were observed when the annealing temperatures is increased to 600 °C (Fig.4a, b, and c). The shape of nanocomposites was confirmed at a particular temperature. The lattice bands of the crystal with spacing (d) is provided by the graphs. HRTEM images reflect unidirectional lattice bands with 0.5 nm as the magnitude of d spacing (Fig. 4c) confirms the crystallinity of the zinc-nickel ferrite system. From the results, it is obvious that at annealing temperature at 600ºC, the zinc-nickel ferrite system nanocomposites declare the shape, nature (crystalline), and structural properties.

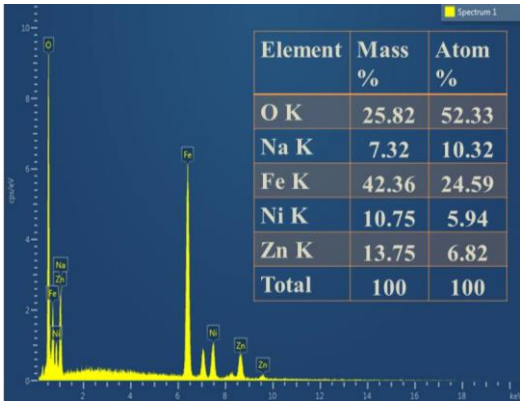

Figure 3. EDX spectra of Zinc Nickel Ferrites Systems (ZNFO NCs) Nanocomposites annealed at 600ºC.

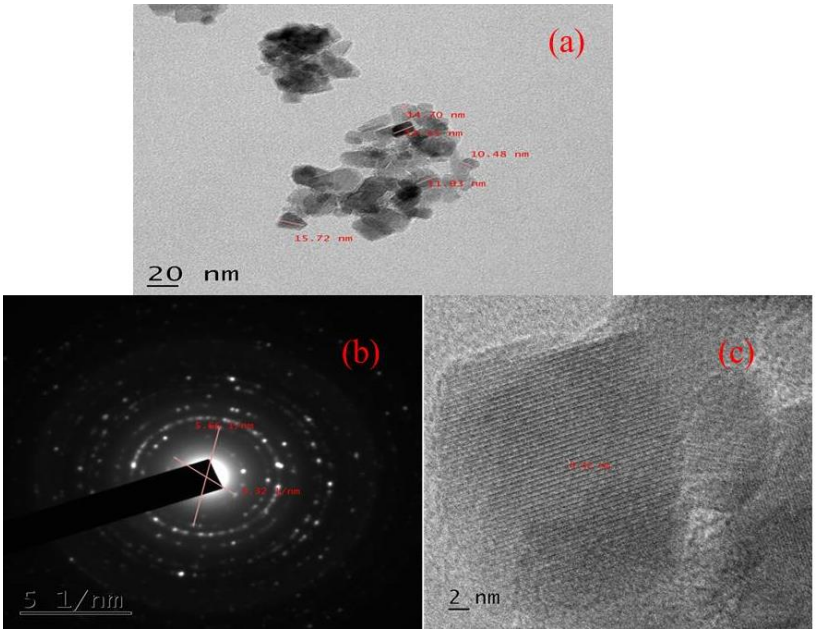

Figure 4. HRTEM images of Zinc Nickel Ferrites Systems (ZNFO NCs) Nanocomposites (a, c) annealed at 600ºC (b) SAED.

3.3. FTIR Spectral measurements.

The FTIR image for Zinc Nickel Ferrites Systems Nanocomposites (ZNFO NCs) is shown in Figure 5. By superimposing the obtained graph for Zinc Nickel Ferrites Systems Nanocomposites (ZNFO NCs) the spectral resemblance is observed. The outcome confirms that the hydroxyl groups are available in the sample, ZNFO NCs. The earlier studies have registered the absence of some hydroxyl ions at specific temperatures. The O-H bonds are visible at 1537.80 – 1500.31 cm^{-1} and 960.03 – 874.235 cm^{-1}, in-plane, and out of a plane, respectively. Due to Fe_3O_4, the spectra of the Zinc Nickel Ferrites systems emphasis a strong band in the region 635.57 - 573.51cm^{-1}[31-32]. The energy band from 635.57 to 573.51 cm^{-1}, may be due to the presence of ZnO, NiO, and Fe_3O_4 [33-35].

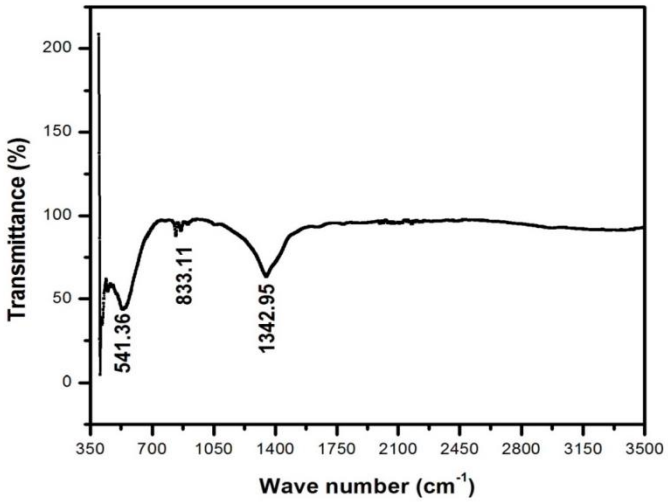

Figure 5. FTIR spectra of Zinc Nickel Ferrites Systems (ZNFO NCs) Nanocomposites.

3.4. Photocatalytic degradation phenomenon of Zinc Nickel Ferrites Systems Nanocomposites (ZNFO NCs).

In this process, 10 mg of cerium oxide powder was dissolved in 10 ml of MB. The mixture is stirred for 2 hours under darkness to achieve adsorption equilibrium. The solution of MB with photocatalyst was analyzed by UV-Vis spectroscopy. Radiation of wavelength 4000-7000 Å is used as the source. The solution was flashed in the solar spectrum during the day at the temperature of 30-33ºC with continuous stirring. The relative concentration of MB in the solution was periodically analyzed by UV-Vis-NIR spectroscopy at an interval of 2 hours. Photocatalytic properties of Zinc Nickel Ferrites Systems Nanocomposites (ZNFO NCs) were studied, and the disintegration of the MB in the aqueous solution under sunlight was also studied. The MB solution is stable under both visible and UV radiation without photocatalyst. To assess the impact of Nickel in the methylene blue degradation, Zinc Nickel Ferrites Systems Nanocomposites (ZNFO NCs) photocatalyst is subjected to photodegradation. From Fig. 6 (a) it is observed that the strong absorption peak located at the wavelength of 647 nm reduces gradually with enhanced exposure time, and absorbance of MB falls drastically after long hours of solar radiation, and it shows better photocatalytic phenomenon. The photocatalytic activity observed for Zinc Nickel Ferrites Systems Nanocomposite (ZNFO NCs) was most effective in MB degradation, with 79% at 8 hours. The photocatalytic activity is proportional to the amount of OH ions on the catalyst. In the absence of illumination, the catalyst shows a small degradation of dyes. It indicates that the catalyst, light, and time of exposure were of prime

importance for rapid dye degradation. The degradation efficiency of the MB aqueous solution is 79% under visible irradiation for 8h using the Zinc Nickel Ferrites Systems Nanocomposites (ZNFO NCs), which emphasis higher photocatalytic activity as acknowledged in Fig. 6 (b).

To analyze the kinetic reaction of MB degradation, the Pseudo-first order relation was applied. The rate of the process is given by the below equation (1)

$$\ln(C_o / C_t) = Kt \text{----------(1)}$$

C_o and C_t are the concentration of the dye at initial and at time t. From the slope of the first order imprint curve, the apparent rate constant k of Zinc Nickel Ferrites Systems Nanocomposites is determined [36-40].

The efficiency of photocatalytic degradation for ZNFO NCs is estimated using the following equation (2).

$$\text{Efficiency} = (Co - Ct)/Co * 100\% \text{----------(2)}$$

The results proclaim that all the photocatalyst shows good MB dye degradation in visible light.

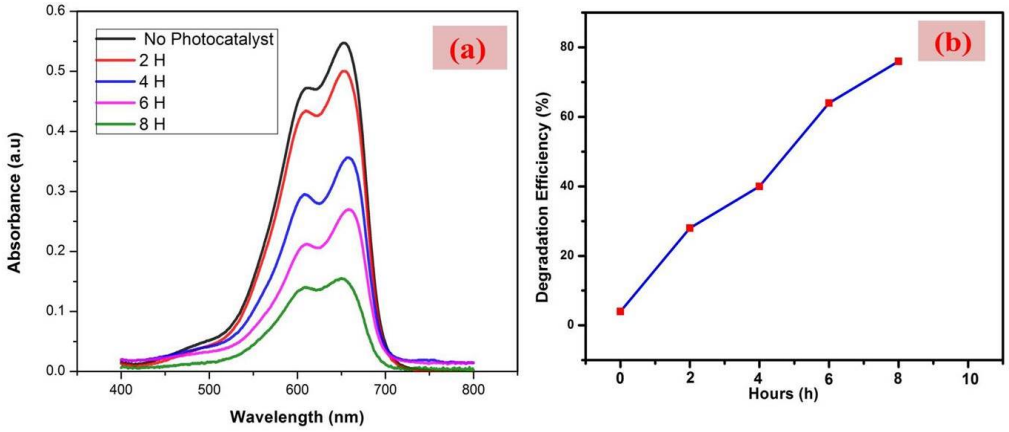

Figure 6. Zinc Nickel Ferrites Systems (ZNFO NCs) Nanocomposites annealed at 600ºC under UV-light irradiation (a) Absorption of MB solution during the photodegradation (b) Photodegradation percentage.

3.5. Measurement of magnetic parameters.

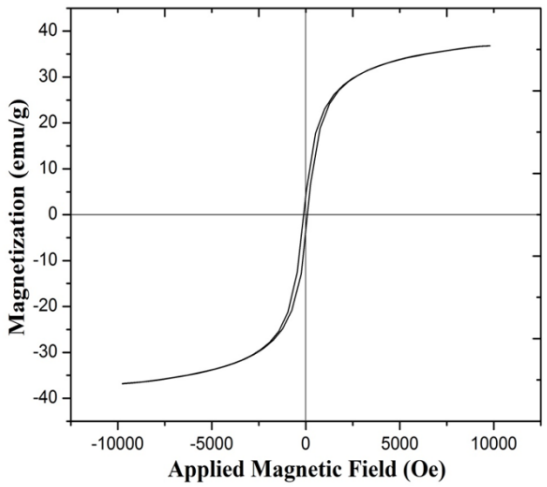

Figure 7. Magnetic hysteresis characterization of Zinc Nickel Ferrites Systems (ZNFO NCs) Nanocomposites.

The arrangement in the cubic ferromagnetic spinel NCs is due to the exceptional exchange mechanism of ions between the regions. The replacement of Zn ion, which has a

fondness of occupying A site, declines the interaction. By enhancing the zinc substitution, it is feasible to modify the magnetic parameters of the crystals. The hysteresis loop of the Zinc-Nickel ferrite system Nanocomposites at room temperature is shown in Fig. 7. The value of the residual magnetization (Mr) 1,999emu/g, the coercivity field (Hc) 31,225 G, and the magnetization at saturation (Ms) 32.225 emu/g are obtained from the graph. The peak value of Ms was derived from the inference curve (H/M versus H). The change in Ms is due to the effect of the cation ratio and their preference in sites of occupancy. The deterioration in the magnetic properties of the nanoparticle may be due to the following aspects like dead layer formation, reduced particle spin [41], non-saturation effects, a divergence of the cation, and presence of water, etc., [42-43]. It is crystal clear that the cation disparity in nanoparticles from its parent material is due to the impact of temperature on magnetization.

4. Conclusions

The preparation of Zinc-Nickel ferrite system Nanocomposites is reported. Zinc-Nickel ferrite system Nanocomposites can be synthesized by the co-precipitation approach. The formation of Nanocomposites was acknowledged by the X-ray diffraction. In the study, the samples obtained by co-precipitation revealed exceptional paramagnetic behavior, and the same was confirmed by the hysteresis curve at room temperature. FTIR confirmed the availability of metal-oxygen bonds and water. The photocatalytic degradation of Zinc-Nickel ferrite system Nanocomposites in MB dye is most effective, and it is found to be 79 % for 8 hours.

Funding

This research received no external funding.

Acknowledgments

The authors thank SAIF KOCHI, India, for extending its instrumental technical supports.

Conflicts of Interest

The authors declare no conflict of interest.

References

1. Kanna, R.R.; Sakthipandi, K.; Lenin, N.; Samuel, E.J.J. Neodymium doped on the manganese–copper nanoferrites: analysis of structural, optical, dielectric and magnetic properties. *Journal of Materials Science: Materials in Electronics* **2019**, *30*, 4473-4486, https://doi.org/10.1007/s10854-019-00736-z.
2. Sasikala, C.; Suresh, G.; Durairaj, N.; Baskaran, I.; Sathyaseelan, B.; Kumar, M.; Senthilnathan, K.; Manikandan, E. Influences of Ti4+ ion on dielectric property in perovskite structure of La ferrite (LaFe1-XTiXO$_3$). *Journal of Alloys and Compounds* **2020**, https://doi.org/10.1016/j.jallcom.2020.155040.
3. Sivakumar,D.; Chandra Babu Naidu,K.; Prem Nazeer,K.; Mohamed Rafi,M.; Ramesh kumar,G.; Sathyaseelan,B.; Killivalavan,G.;Ayisha Begam,A.; Structural Characterization and Dielectric Studies of Superparamagnetic Iron Oxide Nanoparticles, *J. Korean Ceram. Soc.*, **2018**, *55*, 230-238. https://doi.org/10.4191/kcers.2018.55.3.02.
4. Sasikala, C.; Durairaj, N.; Baskaran, I.; Sathyaseelan, B.; Henini, M.; Manikandan, E. Transition metal titanium (Ti) doped $LaFeO_3$ nanoparticles for enhanced optical structural and magnetic properties. *J. Alloys Compd.*, **2017**; *712*, 870-877, https://doi.org/10.1016/j.jallcom.2017.04.133.
5. Jadhav, S.V.; Shewale, P.S.; Shin, B.C.; Patil, M.P.; Kim, G.D.; Rokade, A.A.; Park, S.S.; Bohara, R.A.; Yu, Y.S. Study of structural and magnetic properties and heat induction of gadolinium-substituted manganese zinc ferrite nanoparticles for in vitro magnetic fluid hyperthermia. *Journal of Colloid and Interface Science* **2019**, *541*, 192-203, https://doi.org/10.1016/j.jcis.2019.01.063.

6. Sarac, M.F. Magnetic, Structural, and Optical Properties of Gadolinium-Substituted $Co_{0.5}Ni_{0.5}Fe_2O_4$ Spinel Ferrite Nanostructures. *Journal of Superconductivity and Novel Magnetism* **2020**, *33*, 397-406, https://doi.org/10.1007/s10948-019-05359-3.
7. Anwar, A.; Zulfiqar, S.; Yousuf, M.A.; Ragab, S.A.; Khan, M.A.; Shakir, I.; Warsi, M.F. Impact of rare earth Dy^{+3} cations on the various parameters of nanocrystalline nickel spinel ferrite. *Journal of Materials Research and Technology* **2020**, *9*, 5313-5325, https://doi.org/10.1016/j.jmrt.2020.03.057.
8. Fu, H.; Lin, J.; Zhang, L.; Zhu, Y. Photocatalytic activities of a novel $ZnWO_4$ catalyst prepared by a hydrothermal process. *Appl. Catal. A Gen.***2006**, *306*, 58-67, https://doi.org/10.1016/j.apcata.2006.03.040.
9. Brabers, V.A.M. Comment on Size-dependent Curie temperature in nanoscale $MnFe_2O_4$ particles. *Phys. Rev. Lett.* **1992**, *68*, https://doi.org/10.1103/PhysRevLett.68.3113.
10. Alves, C.R.; Aquino, R.; Depeyrot, J.; Cotta, T.A.P.; Sousa, M.H.; Tourinho, F.A.; Rechenberg, H.R.; Goya, G.F. Surface spin freezing of ferrite nanoparticles evidenced by magnetization measurements. *Journal of Applied Physics* **2006**, *99*, https://doi.org/10.1063/1.2163844.
11. Verveka, M.; Jirak, Z.; Kaman, O.; Knizek, K.; Marysko, M.; Pollert, E.; Zaveta, K.; Lancok, A.; Dlouha, M.;Vratislav, S. Distribution of cations in nanosize and bulk Co–Zn ferrites. *Nanotechnology* **2011**, *22*.
12. Ramos, A.V.; Guittet, M.J.; Moussy, J.B.; Mattana, R.; Deranlot, C.; Petroff, F.; Gatel, C. Room temperature spin filtering in epitaxial cobalt-ferrite tunnel barriers. *Applied Physics Letters* **2007**, *91*, https://doi.org/10.1063/1.2787880.
13. Shankar, S.; Kumar, M.; Ghosh, A.K.; Thakur, O.P.; Jayasimhadri, M. Anomalous ferroelectricity and strong magnetoelectric coupling in $CoFe_2O_4$-ferroelectric composites. *Journal of Alloys and Compounds* **2019**, *779*, 918-925, https://doi.org/10.1016/j.jallcom.2018.11.252.
14. Wu, Y.; Wan, J.; G. Liu, J. M.;Wang, G. Significant enhancement of magnetoelectric output in multiferroic heterostructural films modulated by electric polarization cycles. *Appl. Phys. Lett.* **2010**, *96*, https://doi.org/10.1063/1.3394008.
15. Kim, Y.I.; Kim, D.; Lee, C.S. Synthesis and characterization of $CoFe_2O_4$ magnetic nanoparticles prepared by temperature-controlled co-precipitation method. *Physica B: Condensed Matter* **2003**, *337*, 42-51, https://doi.org/10.1016/S0921-4526(03)00322-3.
16. Li, S.; Liu, L.; John, V.T.; O'Connor, C.J.;Harris, V.G. Cobalt-ferrite nanoparticles: correlations between synthesis procedures, structural characteristics and magnetic properties. *IEEE Trans. Magn*. **2001**, *37*, 2350-2352, https://doi.org/10.1109/20.951169.
17. Didukh, P.; Greneche, J.M.; Ślawska-Waniewska, A.; Fannin, P.C.; Casas, L. Surface effects in $CoFe_2O_4$ magnetic fluids studied by Mössbauer spectrometry. *Journal of Magnetism and Magnetic Materials* **2002**, *242-245*, 613-616, https://doi.org/10.1016/S0304-8853(01)01044-7.
18. Pathmamanoharan, C.; Philipse, A.P. Preparation and Properties of Monodisperse Magnetic Cobalt Colloids Grafted with Polyisobutene. *Journal of Colloid and Interface Science* **1998**, *205*, 340-353, https://doi.org/10.1006/jcis.1998.5589.
19. Rao, C.N.R.; Cheetam, A.K. Science and Technology of Nanomaterials: Current Status and Future Prospects. *J. Mater. Chem.* **2001**, *11*, 2887-2894, https://doi.org/10.1039/b105058n.
20. Fujita, T.; Mamiya, M.; Jeyadevan, B. Basic study of heat convection pipe using the developed temperature sensitive magnetic fluid. *Journal of Magnetism and Magnetic Materials* **1990**, *85*, 203-206, https://doi.org/10.1016/0304-8853(90)90052-R.
21. Auzans, E.; Zins, D.; Blums, E.; Massart, R. Synthesis and properties of Mn-Zn ferrite ferrofluids. *Journal of Materials Science* **1999**, *34*, 1253-1260, https://doi.org/10.1023/A:1004525410324.
22. Ozin, G.A. Nanochemistry: Synthesis in diminishing dimensions. *Advanced Materials* **1992**, *4*, 612-649, https://doi.org/10.1002/adma.19920041003.
23. Singhal, S.; Namgyal, T.; Bansal S.; and Chandra, K. Effect of Zn substitution on the magnetic properties of cobalt ferrite nanoparticles prepared via sol-gel route. *J. Electromagn. Anal. Appl.* **2010**, *2*, 376–381, https://doi.org/10.4236/jemaa.2010.26049.
24. Sinha, M.; Pradhan, S.K. Synthesis of nanocrystalline Cd–Zn ferrite by ball milling and its stability at elevated temperatures. *J. Alloys Compd* **2010**, *489*, 91–98, http://dx.doi.org/10.1016/j.jallcom.2009.09.019.
25. Vestal, C.R.; Zhang, Z.J. Synthesis of $CoCrFeO_4$ nanoparticles using microemulsion methods and size-dependent studies of their magnetic properties, *Chem. Mater*. **2002**, *14*, 3817–3822, https://doi.org/10.1021/cm020112k.
26. Chinnasamy, C.N.; Senoue, M.; Jeyadevan, B.; Perales-Perez, O.; Shinoda, K.; Tohji, K. Synthesis of size-controlled cobalt ferrite particles with high coercivity and squareness ratio. *Journal of Colloid and Interface Science* **2003**, *263*, 80-83, https://doi.org/10.1016/S0021-9797(03)00258-3.
27. Morais, P.C.; Garg, V.K.; Oliveira, A.C.; Silva, L.P.; Azevedo, R.B.; Silva, A.M.L.; Lima, E.C.D. Synthesis and characterization of size-controlled cobalt-ferrite-based ionic ferrofluids. *Journal of Magnetism and Magnetic Materials* **2001**, *225*, 37-40, https://doi.org/10.1016/S0304-8853(00)01225-7.
28. CharlesPrabakar, A.; Sathyaseelan, B.; Killivalavan, G.; Baskaran, I.; Senthilnathan, K.; Manikandan, E.; Sivakumar, D. Photocatalytic Dye Degradation Properties of Zinc Copper Ferrites Nanoparticles. *J. Nanostruct* **2019**, *9*, 694-701, https://doi.org/10.22052/JNS.2019.04.011.

29. CharlesPrabakar, A.; Killivalavan, G.; Sivakumar, D.; Naidu, C.B.; Sathyaseelan.B; Senthilnathan, K.; Baskaran, I.; Manikandan, E.; Rao, R.B.; Sarma, M.S.S.R.K.N.; Ratnamala, A. Structural, morphological, and magnetic properties of copper zinc cobalt ferrites systems nanocomposites. *Biointerface Res Appl Chem.* **2020**, *10*, 6015-6019, https://doi.org/10.33263/BRIAC104.015019.
30. Creanga, D.; Calugaru, G. Physical investigations of a ferrofluid based on hydrocarbons. *Journal of Magnetism and Magnetic Materials* **2005**, *289*, 81-83, https://doi.org/10.1016/j.jmmm.2004.11.023.
31. Dey, S.; Ghose, J. Synthesis, characterisation and magnetic studies on nanocrystalline $Co_{0.2}Zn_{0.8}Fe_2O_4$. *Materials Research Bulletin* **2003**, *38*, 1653-1660, https://doi.org/10.1016/S0025-5408(03)00175-2.
32. Narsimulu, D.; Rao, B.N.; Nagaraju, G.; Yu, J.S.; Satyanarayana, N. Enhanced energy storage performance of nanocrystalline Sm-doped $CoFe_2O_4$ as an effective anode material for Li-ion battery applications. *Journal of Solid State Electrochemistry* **2020**, *24*, 225-236, https://doi.org/10.1007/s10008-019-04484-2.
33. Ma, M.; Zhang, Y.; Yu, W.; Shen, H.-y.; Zhang, H.-q.; Gu, N. Preparation and characterization of magnetite nanoparticles coated by amino silane. *Colloids and Surfaces A: Physicochemical and Engineering Aspects* **2003**, *212*, 219-226, https://doi.org/10.1016/S0927-7757(02)00305-9.
34. Ahmed, S.R.; Kofinas, P. Magnetic properties and morphology of block copolymer-cobalt oxide nanocomposites. *Journal of Magnetism and Magnetic Materials* **2005**, *288*, 219-223, https://doi.org/10.1016/j.jmmm.2004.09.009.
35. Ishikawa, T.; Nakazaki, H.; Yasukawa, A.; Kandori, K.; Seto, M. Influences of Co^{2+}, Cu^{2+} and Cr^{3+} ions on the formation of magnetite. *Corrosion Science* **1999**, *41*, 1665-1680, https://doi.org/10.1016/S0010-938X(98)00198-X.
36. Wu, N.; Fu, L.; Su, M.; Aslam, M.; Wong, K.C.; Dravid, V.P. Interaction of Fatty Acid Monolayers with Cobalt Nanoparticles. *Nano Letters* **2004**, *4*, 383-386, https://doi.org/10.1021/nl035139x.
37. Kale, G.M.; Asokan, T. Electrical properties of cobalt-zinc ferrites. *Applied Physics Letters* **1993**, *62*, 2324-2325, https://doi.org/10.1063/1.109405.
38. Saravanakumar, K.; Ramjan, M.M.; Suresh, P.; Muthuraj, V. Fabrication of highly efficient visible light driven Ag/CeO_2 photocatalyst for degradation of organic pollutants. *Journal of Alloys and Compounds* **2016**, *664*, 149-160, https://doi.org/10.1016/j.jallcom.2015.12.245.
39. Killivalavan, G.; Charles Prabakar, A.; Chandra Babu Naidu, K.; Sathyaseelan, B.; Rameshkumar, G.; Sivakumar, D.; Senthilnathan, K.; Baskaran, I.; Manikandan, E.; Ramakrishna Rao, B. Synthesis and characterization of pure and Cu doped CeO_2 nanoparticles photocatalytic and antibacterial activities evaluation. *Biointerface Res Appl Chem.* **2020**, *10*, 5306-5311, https://doi.org/10.33263/BRIAC102.306311.
40. Asratemedhin B. Habtemariam, Assefu K. Sibhatu, Getu K. Weldegebrieal, Osman A. Zelekew, Belayhun T. Tekletsadik, Bio-mediated synthesis of ZnO nanostructures from Thymus Schimperi leaves extract and its antibacterial and photocatalytic activities, *Letters in Applied NanoBioScience*, **2020**, 9, 808 – 813, https://doi.org/10.33263/LIANBS91.808813.
41. Zhang, L.; Zhang, Q.; Xie, H.; Guo, J.; Lyu, H.; Li, Y.; Sun, Z.; Wang, H.; Guo, Z. Electrospun titania nanofibers segregated by graphene oxide for improved visible light photocatalysis. *Applied Catalysis B: Environmental* **2017**, *201*, 470-478, https://doi.org/10.1016/j.apcatb.2016.08.056.
42. Han, D.H.; Wang, J.P.; Luo, H.L. Crystallite size effect on saturation magnetization of fine ferrimagnetic particles. *Journal of Magnetism and Magnetic Materials* **1994**, *136*, 176-182, https://doi.org/10.1016/0304-8853(94)90462-6.
43. Auzans, E.; Zins, D.; Blums, E.; Massart, R. Synthesis and properties of Mn-Zn ferrite ferrofluids. *Journal of Materials Science* **1999**, *34*, 1253-1260, https://doi.org/10.1023/A:1004525410324.